0026-895X/07/7204-885–896$20.00
MOLECULAR PHARMACOLOGY
Copyright © 2007 The American Society for Pharmacology and Experimental Therapeutics
Mol Pharmacol 72:885–896, 2007

Vol. 72, No. 4
38083/3254655
Printed in U.S.A.

Serotonin 5-Hydroxytryptamine$_{2C}$ Receptor Signaling in Hypothalamic Proopiomelanocortin Neurons: Role in Energy Homeostasis in Females

Jian Qiu, Changhui Xue, Martha A. Bosch, Jonathan G. Murphy, Wei Fan, Oline K. Rønnekleiv, and Martin J. Kelly

Department of Physiology and Pharmacology (J.Q., C.X., M.A.B., O.K.R., M.J.K.), Department of Anesthesiology and Perioperative Medicine (O.K.R.), Center for the Study of Weight Regulation and Associated Disorders (J.G.M., W.F.), Division of Neuroscience, Oregon National Primate Research Center (M.A.B., O.K.R.), Oregon Health & Science University, Portland, Oregon

Received May 22, 2007; accepted July 10, 2007

ABSTRACT

Hypothalamic proopiomelanocortin (POMC) neurons play a critical role in the regulation of energy balance, and there is a convergence of critical synaptic input including GABA and serotonin on POMC neurons to regulate their output. We found previously that 17β-estradiol (E_2) reduced the potency of the $GABA_B$ receptor agonist baclofen to activate G protein-coupled inwardly rectifying potassium (GIRK) channels in hypothalamic POMC neurons through a membrane estrogen receptor (mER) via a Gα_q phospholipase C (PLC)-protein kinase Cδ-protein kinase A pathway. We hypothesized that the mER and neurotransmitter receptor signaling pathways converge to control energy homeostasis. Because 5-HT_{2C} receptors mediate many of the effects of serotonin in POMC neurons, we elucidated the common signaling pathways of E_2 and 5-HT in guinea pigs using single-cell reverse transcription-polymerase chain reaction (RT-PCR), real time RT-PCR, and whole-cell patch recording. Both 5-hydroxytryptamine$_{2C}$ (5-HT_{2C}) and 5-HT_{2A} receptors were coexpressed in POMC neurons. The 5-$HT_{2A/C}$ agonist (±)-1-(2,5-dimethoxy-4-iodophenyl)-2-aminopropane (DOI) desensitized the $GABA_B$ response in a dose-dependent manner, which was antagonized by the selective 5-HT_{2C} receptor antagonists 8-[5-(2,4-dimethoxy-5-(4-trifluoromethylphenylsulphonamido) phenyl-5-oxopentyl]1,3,8-triazaspiro[4.5] decane-2,4-dione hydrochloride (RS102221) and 1,2,3,4,10,14*b*-hexahydro-2-methyldibenzo [*c,f*]pyrazino[1,2-*a*]-azepine hydrochloride (ORG 3363). The 5-HT_{2C} receptor was Gα_q-coupled to PLC activation and hydrolysis of plasma membrane phosphatidylinositol bisphosphate to directly inhibit GIRK channel activity. Coapplication of the two agonists at their EC_{50} concentrations (DOI, 20 μM, and E_2, 50 nM) produced additive effects. Although there was a significant gender difference in the effects of E_2 on baclofen responses, there was no gender difference in 5-HT_{2C} receptor-mediated effects. Finally, both DOI and estrogen (intracerebroventricular) inhibited feeding in ovariectomized female mice. Therefore, the Gα_q signaling pathways of the mER and 5-HT_{2C} receptors may converge to enhance synaptic efficacy in brain circuits that are critical for maintaining homeostatic functions.

This study was supported by United States Public Health Service grants NS43330, NS38809, DK68098, and DK62179.
Article, publication date, and citation information can be found at http://molpharm.aspetjournals.org.
doi:10.1124/mol.107.038083.

The hypothalamus is a key central nervous system center for controlling many homeostatic processes, and hypothalamic POMC neurons are critical neurons in these hypothalamic circuits (Elmquist et al., 1999; Cone, 2005; Gropp et al.,

ABBREVIATIONS: POMC, proopiomelanocortin; E_2, 17β-estradiol; $GABA_B$, γ-amino butyric acid B receptor; GIRK, G protein-coupled inwardly rectifying potassium; mER, membrane estrogen receptor; PLC, phospholipase C; PKCδ, protein kinase C δ; PCR, polymerase chain reaction; PKA, protein kinase A; 5-HT, 5-hydroxytryptamine, serotonin; RT-PCR, reverse transcription-polymerase chain reaction; scRT-PCR, single-cell reverse transcription-polymerase chain reaction; qPCR, quantitative polymerase chain reaction; DOI, (±)-1-(2,5-dimethoxy-4-iodophenyl)-2-aminopropane; RS102221, 8-[5-(2,4-dimethoxy-5-(4-trifluoromethylphenylsulphonamido) phenyl-5-oxopentyl] 1,3,8-triazaspiro[4.5] decane-2,4-dione hydrochloride; ORG 3363, 1,2,3,4,10,14*b*-hexahydro-2-methyldibenzo [*c,f*]pyrazino[1,2-a]azepine hydrochloride, *R*-enantiomer; PIP_2, phosphatidylinositol 4,5 bisphosphate; icv, intracerebroventricular; PVN, paraventricular nucleus; GDX, gonadectomized; BIS, bisindolymaleimide I hydrochloride; DHT, dihydrotestosterone; wortmannin, (1*S*,6br,9a*S*,11*R*,11b*R*) 11-(acetyloxy)-1,6*b*,7,8,9*a*,10,11,11*b*-octahydro-1-(methoxymethyl)-9*a*,11*b*-dimethyl-3*H*-furo [4,3,2-*de*]indeno[4,5,-*h*]-2-*h*-2-benzopyran-3,6,9-trione; spiperone, 8-[4-(4-fluorophenyl)-4-oxobutyl]-1-phenyl-1,3,8-triazaspiro[4,5]decan-4-one hydrochloride; *m*-CPP, 1-(3-chlorophenyl)piperazine hydrochloride; MK212, 6-chloro-2-(1-piperazinyl) pyrazine hydrochloride; aCSF, artificial cerebral spinal fluid; DTT, dithiothreitol; DEPC, diethylpyrocarbonate; MLVRT, murine leukemia virus reverse transcriptase; C_T, cycle threshold; PI, phosphatidylinositol; GAPDH, glyceraldehyde-3-phosphate dehydrogenase; ANOVA, analysis of variance; T, testosterone; IP_3, inositol 1,4,5 triphosphate; DAG, diacylglycerol; U73122, 1-[6-[[17β-methoxyestra-1,3,5(10)-trien-17-yl]amino]hexyl]-1*H*-pyrrole-2,5-dione; U73343, 1-[6-[[17β-3-methoxyestra-1,3,5(10)-trien-17-yl]amino]hexyl]-2,5- pyrrolidine-dione.

2005; Luquet et al., 2005). POMC neurons modulate the excitability of hypothalamic neurons that control reproduction, stress responses, fluid balance, temperature, and appetite through direct synaptic contacts. In addition, POMC neurons project to other brain areas (e.g., midbrain) to control motivated behaviors such as sexual and maternal behavior. There is a heavy projection of serotonin fibers from the dorsal and median raphe nuclei to the arcuate and PVN, and there is a dense expression of 5-HT_{2A} receptors in the PVN and 5-HT_{2C} receptors in the arcuate (Gundlah et al., 1999). Serotonin analogs and drugs that increase the activity of central serotonergic pathways have been developed and widely used as appetite suppressants (Breisch et al., 1976; Bickerdike, 2003). Indeed, the 5-HT reuptake inhibitor/5-HT releaser *d*-fenfluramine and selective 5-HT_{2C} receptor agonists activate α-melanocyte-stimulating hormone-containing neurons (Heisler et al., 2002, 2006), but the cellular mechanism(s) of the 5-HT_{2C} receptor agonist action have not been elucidated.

It is interesting that serotonin neurons are targets of ovarian and testicular steroids (Bethea, 1993). These steroid effects have traditionally been attributed to activation of the nuclear receptors (McEwen, 2001). In nonhuman primates, estrogens up-regulate tryptophan hydroxylase in midbrain 5-HT neurons (Bethea et al., 1998), decrease serotonin transporter mRNA expression in midbrain raphe (Bethea et al., 1998), and decrease expression of the 5-HT_{2C} receptor in a number of hypothalamic nuclei (Gundlah et al., 1999). E_2 modulates many of the homeostatic functions through the transcription factors estrogen receptor-α and -β (Couse and Korach, 1999). However, in contrast to the relatively slow genomic effects of E_2, we have identified a putative mER that is Gα_q-coupled to a PLC-PKC-PKA pathway (Qiu et al., 2003). E_2 reduces the potency of the $GABA_B$ receptor agonist baclofen to activate G-protein-coupled inwardly rectifying K^+ channels in hypothalamic neurons, and this membrane-delimited signaling pathway also plays a critical role in the control of energy homeostasis (Qiu et al., 2006).

It is noteworthy that serotoninergic drugs (i.e., selective serotonin reuptake inhibitors) and E_2 are effective in alleviating postmenopausal symptoms in women (Stearns et al., 2002). It may be that E_2 and serotonin, via mER and 5-HT_{2C} receptors, respectively, synergize to regulate energy metabolism in postpubertal female patients. Therefore, understanding the actions of E_2 and serotonin on POMC neurons may provide insight into fundamental differences between female and male patients in the hypothalamic control of feeding and energy homeostasis. In the present study, we sought to elucidate the cellular cascades activated by 5-HT compared with E_2 in hypothalamic POMC neurons using whole-cell recording, scRT-PCR, and real-time RT-PCR techniques and their functional consequences at the whole animal level. Our findings delineate the 5-HT_{2C} signaling pathway in male and female patients and determine its convergence with the mER signaling pathway in arcuate POMC neurons to control energy homeostasis.

Materials and Methods

Animals and Treatments. All animal procedures described in this study are in accordance with institutional guidelines based on the National Institutes of Health standards. Male and female Topeka guinea pigs (400–600 g), bred in our institutional breeding facility, and female multicolor guinea pigs (400–500 g; Elm Hill Breeding Labs, Chelmsford, MA) were used in these experiments. The guinea pigs were maintained under constant temperature (26°C) and light (on between 6:30 AM and 8:30 PM). Animals were housed individually with food and water provided ad libitum. They were gonadectomized under ketamine-xylazine anesthesia (33 and 6 mg/kg, respectively, s.c.) 5 to 7 days before experimentation and were given sesame oil vehicle (0.1 ml, s.c.) 24 h before experimentation. Serum estrogen concentrations were measured in the GDX female guinea pigs by radioimmunoassay (Oregon National Primate Research Center Radioimmunoassay Core, Beaverton, OR) from trunk blood collected on the day of experimentation and were $<$10 pg/ml. An additional group of female 11- to 12-week-old C57BL/6J mice (The Jackson Laboratory, Bar Harbor, ME) used for feeding study were housed upon arrival on a 12-h light/dark cycle (lights off at 6:00 PM) with free access to standard pellet diet and water.

Drugs. All drugs were purchased from Calbiochem (La Jolla, CA) unless otherwise specified. tetrodotoxin (Alomone Labs, Jerusalem, Israel) was dissolved in Milli-Q H_2O and further diluted with 0.1% acetic acid (final concentration, 1 mM), pH 4 to 5. E_2 was purchased from Steraloids (Wilton, NH), recrystallized to ensure purity, and dissolved in 100% ethanol to a stock concentration of 1 mM. T and DHT (Steraloids) was also dissolved in 100% ethanol. The PKC inhibitors BIS (100 μM) and rottlerin (10 mM), the PLC inhibitor U73122 (20 mM), the less active analog U73343 (20 mM), the PI-4-kinase inhibitor wortmannin (10 mM), RS102221 hydrochloride (10 mM), and spiperone hydrochloride (20 mM; Tocris, Ellisville, MO) were dissolved in dimethyl sulfoxide. Phosphatidylinositol bisphosphate (PIP_2) was dissolved in the pipette solution at concentration of 5 μM. The solution was sonicated intermittently on ice for 30 min. Sonication was repeated each time before filling a new pipette. DOI (20 mM), *m*-CPP (10 mM), MK212 (10 mM), and ORG 3363 (20 mM; Organon NV, Oss, The Netherlands) were dissolved in H_2O. The Gα_q binding protein designed to mimic the C terminus of the Gα_q subunit and the Gα_s binding protein designed to mimic the C terminus of the Gα_s subunit were synthesized by PeptidoGenic Research (Livermore, CA). The peptide sequence for Gα_q peptide was Ac-LGLNLKEYNLV-OH, and the peptide sequence for Gα_s peptide was CRMHLRQYELL. The peptides were also dissolved in H_2O. Aliquots of the stock solutions were stored at $-$20°C until needed.

Electrophysiology. Adult Topeka guinea pigs were gonadectomized 6 to 10 days before each experiment. Each animal was quickly killed by decapitation, the brain rapidly removed from the skull, and a block containing the hypothalamus immediately dissected. The hypothalamic block was submerged in cold (4°C) oxygenated (95% O_2/5% CO_2) aCSF containing the following constituents: 124 mM NaCl, 5 mM KCl, 26 mM $NaHCO_3$, 2.6 mM NaH_2PO_4, 10 mM dextrose, 10 mM HEPES, 2 mM $MgSO_4$, and 2 mM $CaCl_2$ at 4°C. Coronal slices (300–350 μm) through the caudal-rostral extent of the arcuate nucleus were cut with the aid of a vibrating microtome. The slices were transferred to a multiwell auxiliary chamber containing oxygenated aCSF and kept there until electrophysiological recording after ~2 h. During recording, slices were maintained in a chamber perfused via a peristaltic pump with warmed (35°C) oxygenated aCSF at a rate of 1.5 ml/min. Microelectrodes (resistances of 3–6 MΩ) were fabricated from borosilicate glass pipettes (1.5 mm outer diameter) and filled with an internal solution, pH 7.30, containing the following constituents: 128 mM potassium gluconate, 10 mM NaCl, 2 mM $MgCl_2$, 11 mM EGTA, 10 mM HEPES, 1 mM ATP, 0.25 mM GTP, and 0.25% biocytin. Standard whole-cell, voltage-clamp procedures were followed using an Axopatch 200A amplifier (Molecular Devices, Sunnyvale, CA). Signals were digitized with a Digidata 1200 and analyzed using pClamp 7.0 software (Molecular Devices). The liquid junctional potential of $-$10 mV was corrected in the data analysis. Current and voltage traces were also recorded on an analog chart recorder (Gould Instrument Systems, Cleveland, OH). After the formation of a $>$1 GΩ seal, intracellular access was achieved by suction, and only those cells that

showed less than 10% change in access resistance throughout the recording were included in this study. All of the responses to baclofen were measured in voltage clamp as outward currents (V_{hold} = −60 mV). For the electrophysiology analysis, only cells with gigaohm or better seals were included in this study.

The protocol for drug administration in the whole-cell patch voltage-clamp experiments (V_{hold}, −60 mV) was followed as described in a previous publication (Qiu et al., 2003). After seals were formed and the whole-cell configuration was obtained, slices were perfused with tetrodotoxin (1 μM) for 5 min. The first $GABA_B$ receptor-mediated response was generated by perfusing baclofen (at EC_{50} concentration of 5 μM) until a steady-state outward current was obtained (R_1). After drug washout, the current returned to its predrug resting level. The cells were then treated with serotonin receptor agonist drugs DOI and/or other drugs for 15 min, baclofen (5 μM) was perfused again, and R_2 was measured. The effects of serotonin receptor agonist drugs or other drugs on the baclofen response are expressed as a percentage of R_2 over R_1.

Composite dose-response curves were generated from the following logistic equation fitted by computer (Sigma Plot 8.0; SPSS Inc., Chicago, IL) to the data: $\Delta I_{max} = 100 \times ([agonist]^{nH}/([agonist]^{nH} + EC_{50}{}^{nH}))$, where ΔI_{max} is the maximum outward current for a given agonist, EC_{50} represents the agonist potency, and n_H is the Hill slope.

Immunocytochemistry. After electrical recording, the slices were prepared for fluorescence immunocytochemistry as described previously (Qiu et al., 2003). In brief, the slices were fixed with 4% paraformaldehyde in Sorensen's phosphate buffer, pH 7.4, for 120 min, immersed overnight in 20% sucrose dissolved in Sorensen's buffer, and frozen in OCT embedding medium (Sakura Finetek, Torrance, CA) and prepared for immunocytochemistry as described previously (Kelly and Rønnekleiv, 1994). In brief, coronal sections (20 μm) were cut on a cryostat (model 1720 Digital Cryostat; Leitz, Wetzlar, Germany) and mounted on Fisher SuperFrost Plus slides (Fisher Scientific Co., Pittsburgh, PA). Sections were washed for 5 min with 0.1 M sodium phosphate buffer, pH 7.4, and then streptavidin-Cy2 (1:7500–1:10,000; Jackson ImmunoResearch Laboratories Inc., West Grove, PA) was applied for 2 h. The reaction was terminated by washing with buffer. The slices were scanned for the injected neuron with a Nikon (Melville, NY) Eclipse 800 fluorescence microscope. After localization of the biocytin-filled neurons, the slides containing the appropriate sections were processed for the presence of β-endorphin using fluorescence immunohistochemistry as described previously (Kelly and Rønnekleiv, 1994). In brief, the sections with the biocytin-identified neurons were incubated overnight with a polyclonal β-endorphin antibody (kindly provided by Dr. Robert Eskay, National Institutes of Health, Bethesda, MD) at 1:5000 and washed in 0.1 M phosphate buffer followed by incubation with a donkey anti-rabbit IgG-Cy3 at 1:500 (Jackson ImmunoResearch Laboratories Inc.). The sections were washed with sodium phosphate buffer, and coverslips were applied using a glycerolglycine buffer (2:1), pH 8.6, containing 5% *N*-propylgallate (Sigma-Aldrich, St. Louis, MO) to reduce photobleaching. Immunostained cells were analyzed and photographed using a Nikon E800 microscope.

Dispersed Single-Cell RT-PCR. Arcuate single-cell harvest from guinea pig hypothalamic slices was performed as described previously (Qiu et al., 2003). In brief, coronal hypothalamic slices (350 μm) were cut on a vibrating microtome and placed in an auxiliary chamber containing oxygenated aCSF. The slices were allowed to recover for 1 to 2 h in the chamber before dispersion. The arcuate nucleus of the hypothalamus was microdissected and incubated in 2 to 3 ml of aCSF containing 1 mg/ml protease XIV (Sigma-Aldrich) for ~15 min at 37°C. The tissue was then washed three times in 1 volume of low-calcium aCSF and two times in normal aCSF. The cells were isolated by trituration with flame-polished Pasteur pipettes, dispersed on a dish, and perfused continuously with aCSF at a rate of 1.5 ml/min. Cells were visualized using a Nikon inverted microscope, and individual neurons were patched and harvested into the patch pipette by applying negative pressure. The content of the pipette was expelled into a siliconized microcentrifuge tube containing 5 μl of the following solution: 0.5 μl of 10× buffer (100 mM Tris-HCl, 500 mM KCl, and 1% Triton X-100; Promega, Madison, WI), 15 U of RNasin (Promega), 0.5 μl of 100 mM DTT, and DEPC-treated water (Ambion, Austin, TX). In addition, hypothalamic tissue was homogenized, and total RNA was extracted using the RNeasy kit (QIAGEN, Valencia, CA) according to the protocol of the manufacturer. The harvested cell solution and 25 ng of hypothalamic total RNA in 1 μl were denatured for 5 min at 65°C and cooled on ice for 5 min, and then single-stranded cDNA was synthesized from cellular RNA by adding 50 U of MLVRT (Applied Biosystems, Foster City, CA), 1.5 μl of 10× buffer, 2 mM $MgCl_2$, 0.2 μl of dNTPs, 15 U of RNasin, 10 mM DTT, 100 ng of random hexamers (Promega), and DEPC-treated water to a final volume of 20 μl. Cells and tissue RNA used as negative controls were processed as described above but without MLVRT. The reaction mixtures were incubated at 42°C for 60 min, denatured at 99°C for 5 min, and cooled on ice for 5 min.

TABLE 1
Primer sequences used for single-cell RT-PCR and qPCR
The sense primer is listed first with the antisense primer below.

Name	Product Length	Primer Sequence	Base PairNo.	Accession No.
	bp			
POMC[a]	206	TTGCTGGCCCTCCTGCTTCA	37–57	S78260
		CTCTCGGCTCTTCTTATCTG	251–231	
5-HT$_{2C}$[a]	252	GCACCATGCCAGGCTATCAAC	1–21	EF212439
		GTTGGAGAAAGCCCTGCGGTA	252–232	
5-HT$_{2A}$[a]	348	ACCGCTATGTTGCCATCCAGAA	80–101	M85162
		AATGGTTGTCAGGGTGATCAG	427–406	
5-HT$_{1A}$[a]	302	TCCGACGTGACCGTCAGCTA	85–104	AF488978
		AATGGTTGTCAGGGTGATCAG	386–367	
GAPDH[b]	212	CATCCACTGGTGCTGCCAAG	123–142	CPU51572
		GTCCTCGGTGTAGCCCAAGA	334–315	
5-HT$_{2C}$[c]	146	TATCGCTGGATCGGTATG	151–168	EF620035
		ATCCCTCAGTCCAATCAC	296–279	
5-HT$_{2A}$[c]	100	CCATAGCCGCTTCAACTC	111–129	M85162
		CAGCCCAAAGACTGGAAC	210–193	
5-HT$_{1A}$[c]	92	TCGGTTCCTTGGCGGTTAC	107–125	EF620034
		GCCCAGAGTCCACTTGTTGAG	198–178	

bp, base pair(s).
[a] Primers used for single-cell RT-PCR.
[b] Primers used for both single-cell and qPCR.
[c] Primers used for qPCR.

Primers listed in Table 1 were designed using the Clone Manager Software (Scientific and Educational Software, Cary, NC) and synthesized by Invitrogen (Carlsbad, CA). PCR was performed using 3 μl of cDNA template (2 μl for GAPDH) from each RT reaction in a 30 μl of PCR reaction volume containing the following: 3 μl of 10× buffer, 2.4 μl of 25 mM $MgCl_2$ (2 mM final concentration), 0.2 mM dNTPs, 0.2 μM forward and reverse primers, 2 U of TaqDNA polymerase (Promega), and 0.22 μg of TaqStart antibody (Clontech, Mountain View, CA). TaqDNA polymerase and TaqStart antibody were combined and incubated at room temperature for 5 min, and the remainder of the reaction contents was added to the tube and incubated at 94°C for 2 min. PCR reactions for 5-HT_{1A}, 5-HT_{2A}, and 5-HT_{2C} went through 42 to 47 cycles of amplification according to the following protocols: 20-s denaturation (94°C), 30-s annealing (59–62°C), 30-s elongation (72°C), with a final 72°C extension for 5 min. POMC and GAPDH PCR went through 45 and 37 cycles of amplification, respectively, in two steps: 30-s denaturation (94°C), 45-s annealing (65–67°C), with a final 72°C extension for 5 min. Ten microliters of the PCR products were visualized with ethidium bromide on a 1.5% agarose gel.

Real-Time RT-PCR. Total RNA was extracted from the microdissected arcuate nucleus of GDX female guinea pigs (n = 6) using the RNAqueous-Micro kit (Ambion). The RNA was treated with DNase I using the DNA-free kit (Ambion) according to manufacturer's instructions and quantified using the NanoDrop spectrophotometer (NanoDrop Technologies, Wilmington, DE). Reverse transcription was carried out with 200 ng of total RNA using 50 U RT (Applied Biosystems), 1.5 μl of 10× buffer, 2 mM $MgCl_2$, 0.2 mM dNTPs, 15 U of RNasin, 10 mM DTT, 100 ng of random hexamers, and DEPC-treated water to a final volume of 20 μl. As a negative control, RNA was processed as described above but without MLVRT. The reaction mixtures were incubated at 42°C for 60 min, denatured at 99°C for 5 min, and cooled on ice for 5 min.

qPCR was performed using an equivalent of 1.5 ng of total RNA (3 μl of a 1:20 dilution of cDNA template), 0.5 μM forward and reverse primers, and the Power SybrGreen PCR Master Mix (Applied Biosystems) in a 20-μl reaction volume. The qPCR reaction for 5-HT_{2C}, 5-HT_{2A}, 5-HT_{1A}, and GAPDH contained 10 μl of 2× Master Mix, 0.5 μM forward and reverse primers, 3 μl of cDNA, and nuclease-free water to a 20 μl final volume. qPCR was performed on samples in the ABI Prism 7500 Fast machine in triplicate under the following conditions: 95°C, 10 min; 40 cycles of amplification at 95°C, 15 s, and 60°C, 1 min followed by a dissociation step for melting point analysis with 35 cycles of 95°C for 15 s, 60°C to 95°C in increments of 1°C for 1 min, and 95°C for 15 s. Standard curves using diluted cDNA from guinea pig hypothalamus (1:5, 1:10, 1:50, 1:100, 1:500) (Fig. 6e) were prepared to determine the efficiency of the primers. The slopes of the standard curves for 5-HT_{2C}, 5-HT_{2A}, 5-HT_{1A}, and GAPDH were −3.1, −3.2, −3.2, and −3.3, respectively (Fig. 6e). The efficiency was calculated for each primer pair using the following formula: $E = 10^{(-1/m)} - 1$, where m = slope (Livak and Schmittgen, 2001; Pfaffl, 2001). The efficiencies were 100% for all transcripts. The similar efficiencies between the primer pairs allowed us to make quantitative estimates between 5-HT_{2C}, 5-HT_{2A}, and 5-HT_{1A} mRNA expression. The amplification data were analyzed by the ABI 7500 System version 1.3.0 software and calculated using the $\Delta\Delta C_T$ method (Livak and Schmittgen, 2001).

For quantification of 5-HT_{2C}, 5-HT_{2A}, and 5-HT_{1A} receptor mRNA, expression differences were analyzed using qPCR. The $\Delta\Delta C_T$ method was used to calculate relative mRNA expression (Livak and Schmittgen, 2001). 5-HT_{2C}, 5-HT_{2A}, and 5-HT_{1A} receptor mRNA values were normalized to the endogenous control gene GAPDH. 5-HT_{2C} was used as the calibrator and as a reference to which 5-HT_{2A} and 5-HT_{1A} were compared. The relative target gene expression was calculated using $2^{-\Delta\Delta C_T}$, where ΔC_T = target C_T − control C_T, $\Delta\Delta C_T = \Delta C_T$ target − ΔC_T calibrator. Mean and S.E.M. were calculated using Prism 4 software (GraphPad Software Inc., San Diego, CA).

Feeding Study. Eleven- to twelve-week-old female mice anesthetized by intraperitoneal injection of 0.15 ml of mouse cocktail (ketamine-xylazine-saline, 1:1:8) were ovariectomized and then kept anesthetized with isoflurane during the icv cannulation procedure. The mice were placed into a stereotaxic instrument (Cartesian Instruments, Bend, OR), the cranial surface cleaned, and a cannula placed into the third ventricle as described previously (Cepoi et al., 2004). In brief, a small hole was drilled, and a sterile stainless steel guide cannula (25 gauge, 1.1 cm long, with an obturator stylet placed within) was implanted at midline, 0.825 mm posterior to bregma and 4.8 mm below bregma based on Franklin and Paxinos (1997). Mice were housed individually and allowed to recover for 10 days. Thereafter, the animals were adapted repeatedly for at least 3 weeks to the experimental procedure, which included a brief restraint in a procedure bag during which time the icv injection was performed. To test the effects of the compounds on feeding after an overnight fast, mice were placed in clean cages with bedding material and free access to water but without food for 16 h (5:00 PM to 9:00 AM). At the end of the fast, each mouse was lightly restrained, the obturator stylet was removed from the guide cannulae, and saline (0.9% NaCl), E_2 (0.012 nmol) or DOI (110 nmol) in 2-μl total volume was infused over a 1-min period. Another 1-min period was allowed for diffusion of the drugs before removing the injection needle. The mice were put back into their cages with a preweighed food pellet (Purina Mouse Chow, 5144; Purina, St. Louis, MO). Body weight and pellet weights were determined at 1, 2, 6, and 24 h after injection. The correct cannulae placement was confirmed by injecting methylene blue dye at the end of the study and visualizing the location of the dye in brain slices.

Statistical Analysis. Comparisons between groups were performed using a one-way or two-way ANOVA and Bonferroni post test for the tissue analysis and whole-animal experiments and a one-way ANOVA for the electrophysiological experiments with post hoc Newman-Keuls paired analysis. Differences were considered statistically significant if the probability of error was <5%.

Results

Gender Differences in the Estrogen-Mediated Desensitization of the $GABA_B$ Response in Hypothalamic Neurons. Whole-cell recordings were made in arcuate neurons (n = 153) from GDX male and female guinea pigs. A subgroup of these neurons (n = 56) was identified using dual-labeling immunocytochemistry (Fig. 1), and 40% of the neurons were β-endorphin-positive (i.e., POMC neurons). For the electrophysiology analysis, only cells with gigaohm or better seals were included in this study. There was no difference in the mean resting membrane potential (male guinea pigs: −55.5 ± 1.3 mV (n = 21) versus female guinea pigs: −55.0 ± 0.5 mV (n = 102), I_{hold} = 0 pA) or the mean input resistance (male guinea pigs: 0.96 ± 0.3 GΩ versus female guinea pigs: 0.92 ± 0.1 GΩ) between the two groups. Similar to our previous findings in mice (Qiu et al., 2006), there were no gender differences in the mean outward current induced by 5 μM baclofen (male mice: 37.7 ± 3.8 pA, n = 43; female mice: 34.7 ± 2.4 pA, n = 88). However, there was a significant gender difference in the effects of E_2 on the baclofen response in GDX guinea pigs. POMC neurons from GDX male guinea pigs were less sensitive to the effects of estrogen by approximately 15% (Fig. 1). T at a higher concentration (1 μM) could attenuate the baclofen response (Fig. 1, a and b) in GDX male guinea pigs but still was not as efficacious as E_2. However, DHT (1 μM), which cannot be aromatized to E_2, had no effect on the baclofen response (Fig. 1, a and b), suggesting an estrogenic response.

Activation of the 5-HT$_{2C}$ Receptor Desensitized the GABA$_B$ Response in Male and Female POMC Neurons. The anorectic effects of serotoninergic drugs are believed to act via increasing the activity of POMC cells. 5-HT$_{2C}$ agonists (*m*-CPP and MK212) increase the firing frequency of male POMC neurons (Heisler et al., 2002), but the cellular signaling pathways mediating serotonin's effects are not known. However, the attenuation of the prominent GABA and opioid inhibitory input through the uncoupling of $G_{i/o}$ receptors from GIRK channels might account for the increase in POMC neuronal firing after exposure to serotonin-specific 5-HT$_{2A/C}$ agonists (Heisler et al., 2002). In this experiment, we used the whole-cell recording method to measure the effects of DOI on the activation of the GIRK conductance by the GABA$_B$ receptor agonist baclofen. For assessing DOI modulation of the GABA$_B$ response, we used an EC_{50} concentration (5 μM) of baclofen and the protocol described previously (Qiu et al., 2003). A robust outward current was measured in response to baclofen that subsided after washout of the GABA$_B$ agonist (Fig. 2a). The application of baclofen 20 min later elicited the same robust response, suggesting that desensitization and rundown were not occurring in response to successive applications of 5 μM baclofen. However, if DOI (20 μM) was applied during the interim period (i.e., after the washout of the first application of baclofen), there was a significant ($p < 0.01$) decrease of 30% in the response to a second application of baclofen (Fig. 2a). DOI alone had no effect on the holding potential, and current-voltage relationships generated before and during the application of DOI (20 μM) showed that this drug did not change the reversal po-

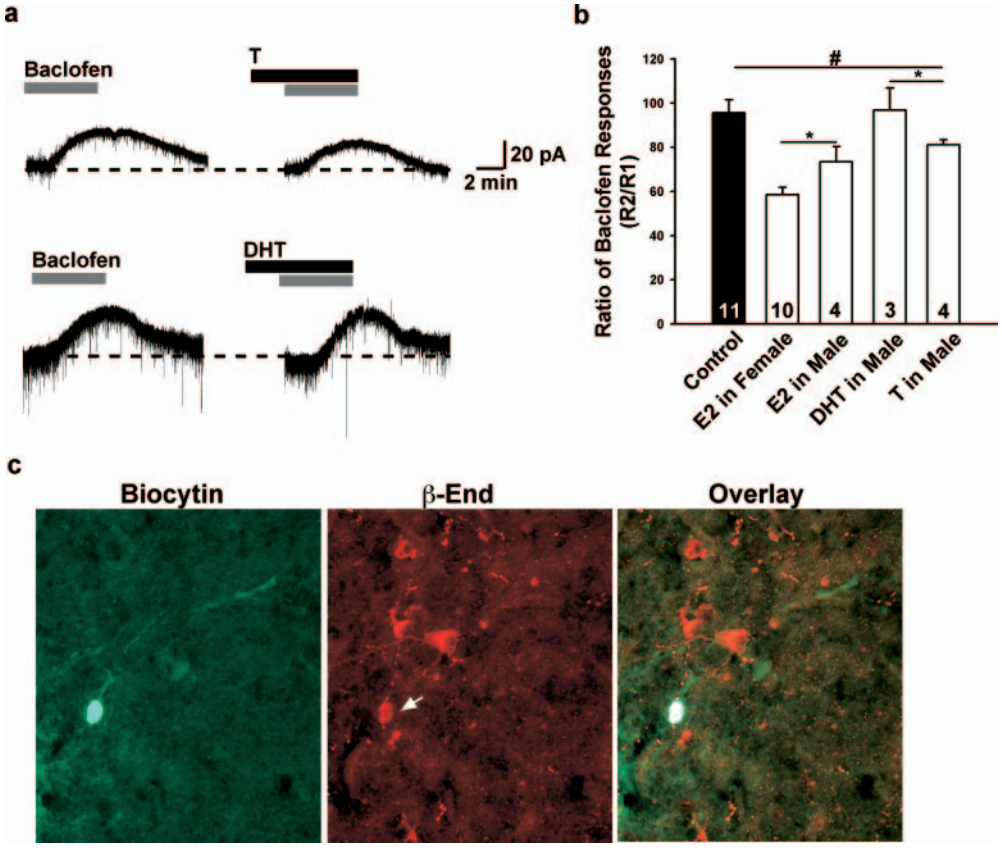

Fig. 1. Gender differences in the effects of E_2 on baclofen responses in GDX guinea pigs. a, representative traces of the baclofen response in the presence of T (1 μM) or DHT (1 μM) in male arcuate (POMC) neurons. b, bar graphs summarizing the effects of the E_2 (100 nM), T (1 μM), and DHT (1 μM) in arcuate (POMC) neurons. E_2 was more effective in female than in male arcuate (POMC) neurons. T at a higher concentration (1 μM) could mimic, but DHT could not mimic the effects of E_2. Bars represent the mean ± S.E.M. of 3 to 11 cells tested per group. *, $p < 0.05$, E_2 in female versus male neurons, and DHT versus testosterone in male neurons; #, $p < 0.05$, T versus control. Because there was no difference in female (96.6 ± 6%, $n = 8$) and male (96.0 ± 5%, $n = 3$) control cells, the data were combined for the control bar. c, a representative POMC neuron that responded to DOI. Arcuate neurons were filled with biocytin during the whole-cell recording. Left, biocytin-streptavidin-Cy$_2$ labeling of a small fusiform arcuate neuron. Scale bar, 20 μm. Middle, immunocytochemical staining of β-endorphin in the same neuron (arrow). Right, overlay of stains shown left and middle.

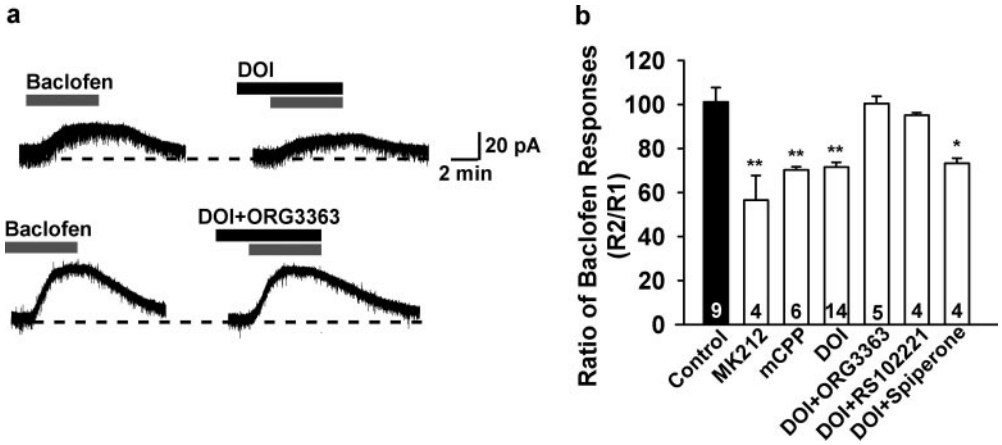

Fig. 2. Activation of 5-HT$_{2C}$ receptors desensitizes the GABA$_B$ response in POMC neurons. a, representative traces of the effects of DOI and ORG 3363 on the baclofen responses. b, bar graphs summarizing the effects of 5-HT$_{2C}$ receptor agonists MK212 (10 μM) and *m*-CPP (10 μM), 5-HT$_{2A/C}$ receptor agonist DOI (20 μM), 5-HT$_{2A}$ receptor antagonist spiperone (20 μM), and 5-HT$_{2C}$ receptor antagonists ORG 3363 (10 μM) and RS102221 (20 μM). Bars represent the mean ± S.E.M. of 4 to 14 cells. *, $p < 0.05$, and **, $p < 0.01$, versus vehicle control.

tential for the baclofen-mediated response: control $E_{baclofen}$, -92.7 ± 2.3 mV, $n = 11$; versus after DOI, $E_{baclofen}$, -95.1 ± 3.7 mV, $n = 11$. In addition, both 5-HT_{2c} receptor agonist MK212 and 5-$HT_{2C/1B}$ receptor agonist *m*-CPP also could significantly inhibit the baclofen response and even gave a more robust inhibition (40%) of the baclofen response. Furthermore, the effects of DOI were blocked by the 5-HT_{2C} receptor antagonists ORG 3363 (10 μM) or RS102221 (20 μM) but not the 5-HT_{2A} receptor antagonist spiperone (20 μM) when coperfused with DOI (Fig. 2, a and b). Treatment with ORG 3363, RS102221, or spiperone alone had no effect on the baclofen response (data not shown). In contrast to the gender differences in the E_2 densensitization of the $GABA_B$ response, there was no difference between male and female POMC neurons in the DOI-mediated effects (71.5 $\pm$ 2.3, R_2/R_1, $n = 13$, for female versus 78.7 $\pm$ 1.7, R_2/R_1, $n = 4$, for male POMC neurons). Therefore, we characterized the signaling pathway of the 5-HT_{2C} receptor in female arcuate (POMC) neurons.

5-HT_{2C} Receptor-Mediated Attenuation of the $GABA_B$ Response Was Dependent on Activation of Gα_q. Early studies showed that 5-HT_2 receptor subtypes couple to Gα_q protein and activate PLC (de Chaffoy de Courcelles et al., 1985; Conn et al., 1986). Therefore, we next examined the involvement of specific signaling proteins in the DOI-mediated modulation. Because 5-$HT_{2A/C}$ receptors are Gα_q protein-coupled and PKC is the downstream pathway, we first examined whether activation of PKC is critical for DOI modulation of the $GABA_B$ response using a PKC inhibitor. If activation of the PKC pathway is involved, then the effect of DOI on $GABA_B$ responses should be blocked by inhibiting PKC. To test this, we applied a PKC inhibitor, BIS, which is a selective inhibitor of PKC that does not distinguish between the conventional, novel, and atypical isoforms of PKC, and a selective PKCδ inhibitor, rottlerin. We have established that BIS (100 nM) and rottlerin (5 μM) block the inhibition of baclofen responses by E_2 (Qiu et al., 2003). But as shown in Fig. 3, after ~15 min of dialysis with BIS (100 nM), the DOI-induced reduction of the $GABA_B$ response was not attenuated. Furthermore, both BIS (100 nM) and rottlerin (5 μM) did not block the inhibition of baclofen response by *m*-CPP, a selective 5-HT_{2C} agonist ($p > 0.05$, *m*-CPP, 71.17 $\pm$ 2.24, $n = 3$, versus *m*-CPP + BIS, 73.16 $\pm$ 3.06, $n = 7$; *m*-CPP versus *m*-CPP + rottlerin 68.92 $\pm$ 4.01, $n = 3$). These results indicate that the suppression of the $GABA_B$ response by DOI requires PLC activation but not the activation of PKC. To examine whether the DOI-mediated inhibition of the $GABA_B$ response depended on the activation of Gα_q, arcuate neurons were dialyzed with a peptide (11 amino acids) that mimics the C-terminal binding site of Gα_q. A similar strategy has been used by Carr et al. (2002) to abro-

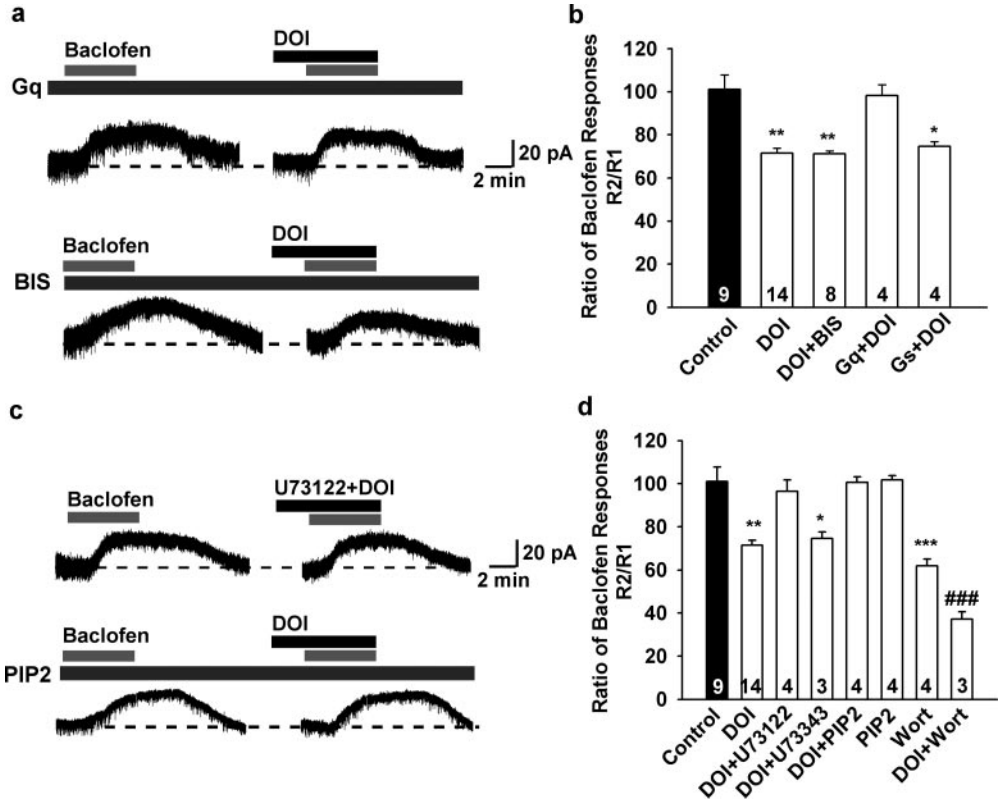

Fig. 3. 5-HT_{2C} receptor-mediated attenuation of the $GABA_B$ response depends on activation of Gα_q but not PKC. Cells were dialyzed for 15 min before baclofen application with BIS (100 nM), Gα_q (200 μM), or Gα_s peptide (200 μM), which were included in the patch pipette solution. a, representative traces of the baclofen responses in the presence of PKC inhibitor BIS or Gα_q peptide. b, bar graphs summarizing the effects of the broad-spectrum PKC inhibitor BIS and Gα inhibitors. Bars represent the mean $\pm$ S.E.M. of 4 to 14 cells. *, $p < 0.05$, Gα_q peptide plus DOI versus Gα_s peptide plus DOI; and **, $p < 0.01$ versus vehicle control. c and d, 5-HT_{2C} receptor-mediated attenuation of the $GABA_B$ response depends on activation of PLC. c, representative traces of the baclofen responses in the presence of PIP_2 or the PLC inhibitor U73122. Cells were dialyzed for 15 min before baclofen application with PIP_2 (5 μM), which was included in the patch pipette solution. d, bar graphs summarizing the effects of PIP_2, PLC inhibitor U73122 (10 μM) and the inactive analog of U73122, U73343 (10 μM), and PI-4-kinase inhibitor wortmannin (wort, 10 μM). Bars represent the mean $\pm$ S.E.M. of 3 to 14 cells. *, $p < 0.05$, U73122 plus DOI versus U73343 plus DOI; **, $p < 0.01$ versus vehicle control; ***, $p < 0.005$ versus vehicle control; and ###, $p < 0.005$ Wort versus DOI plus Wort.

gate 5-HT$_2$ receptor signaling in prefrontal cortical neurons. Indeed, in cells dialyzed with this peptide (200 μM), the DOI-mediated reduction of the GABA$_B$ response was blocked significantly (Fig. 3, a and b) compared with cells dialyzed with a control peptide (11 amino acids) that mimics the C-terminal domain of Gα_s (Fig. 3, a and b).

Desensitization of GABA$_B$ Response Was Dependent on 5-HT$_{2C}$ Activation of PLC and Hydrolysis of Plasma Membrane PIP$_2$. In light of the above results for a primary role for Gα_q in DOI-mediated inhibition, we tested whether the activation of PLC might also play a role. Because the specific PKC inhibitor BIS did not block the effects of DOI, this indicated that the PLC, which is downstream from the activation of Gα_q protein and a well known Gα_q effector, may be responsible for the DOI effect. Therefore, we focused on pathways downstream of PLC to further elucidate the DOI-mediated signaling pathway. To determine whether the activation of PLC is required for the DOI-induced inhibition of the GABA$_B$ response, neurons were treated with the broad-spectrum PLC inhibitor U73122 (10 μM), which was perfused in the extracellular bathing media. Under these conditions, there was no difference between the first baclofen response and second one in the presence of U73122 (U73122-treated versus control group, 95.57 $\pm$ 2.44, $n = 3$ and 96.48 $\pm$ 5.9, $n = 5$), but the DOI-mediated reduction of GABA$_B$ response was blocked (Fig. 3, c and d), whereas the less active PLC inhibitor U73343 at the same concentration had no effect (Fig. 3, c and d). Furthermore, whole-cell dialysis with PIP$_2$ (5 μM) also attenuated the DOI-mediated inhibition, and there were no significant differences between the first baclofen responses with and without PIP$_2$ dialysis. Moreover, the addition of PI-4-kinase inhibitor wortmannin at 10 μM potentiated the inhibition of DOI on the baclofen response (Fig. 3d). Therefore, the 5-HT$_{2C}$ receptor signals through PLC and PIP$_2$, which is different from the mER signaling pathway (Qiu et al., 2003). Because DOI and E$_2$ act through divergent Gα_q signaling pathways, we investigated the convergence of the 5-HT$_{2A/C}$ receptor agonist DOI and E$_2$ on the GABA$_B$ response. Concentration-response curves (Fig. 4b) showed that DOI rapidly attenuated the GABA$_B$ response in a concentration-dependent manner with 50% inhibition at 16.5 μM for DOI. Therefore, based on the previously published EC$_{50}$ value (46.0 nM) for the E$_2$-mediated desensitization of the GABA$_B$ response (Qiu et al., 2006), we coapplied both agonists at their EC$_{50}$ concentrations and found that the effects were additive (Fig. 4, a and c).

5-HT$_{2A/C}$ Receptor Agonist DOI and Estrogen Reduced Food Intake and Body Weight in GDX Female Mice. As proof of principle that the mER and serotonin 5-HT$_{2C}$ signaling pathways are physiologically important, we investigated the short-term effect of DOI and E$_2$ in attenuating the weight gain in the female (Fig. 5). Female mice were ovariectomized, allowed to recover for 10 days, and, thereafter, were adapted repeatedly to the icv injection procedure as described under *Materials and Methods*. Changes in food intake and body weight gain were measured after overnight food deprivation. Based on a dose-response to DOI (10, 20, and 110 nM), no effect was observed with 10 nM. After 20 nM DOI, inhibition of food intake ($p < 0.05$) but not body weight gain was observed at 6 h (data not shown). After 110 nM DOI, food intake and body weight gain were strongly inhibited starting already at 1 h after DOI injection compared with saline, vehicle controls (Fig. 5, a and b; $p < 0.05$–0.005). The greatest effects on body weight and food intake after DOI treatment were observed at 6 h. At that time point, similar to DOI, E$_2$, albeit at a significantly lower dose, attenuated the weight gain and food intake in GDX female mice (Fig. 5, c and d).

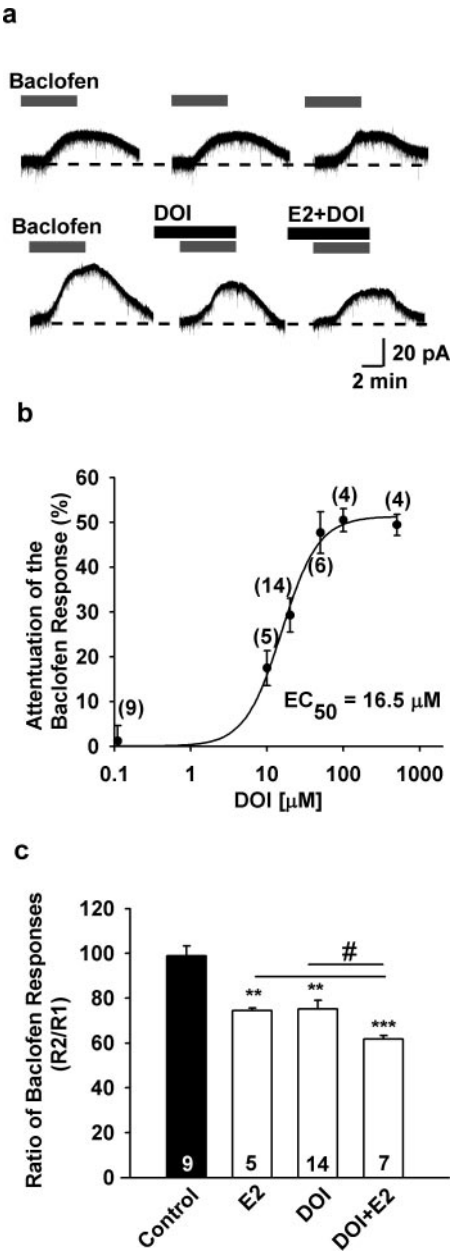

Fig. 4. Effects of DOI and E$_2$ on GABA$_B$ response were additive. a, representative traces of the baclofen response in the absence or presence of DOI (20 μM) alone or DOI plus E$_2$ (50 nM) in arcuate (POMC) neurons. b, cells were perfused with different concentrations of DOI (0, 10, 50, 100, and 300 μM). Data are presented as mean $\pm$ S.E.M. ($n = 4$–14 cells/data point). Based on a logistics equation fit to the data points (see *Materials and Methods*), the EC$_{50}$ value of the inhibition of baclofen response by DOI was 16.5 μM. The Hill slope for DOI was 1.8. c, bar graphs summarizing the effects of DOI (20 μM) and E$_2$ (50 nM). E$_2$ or DOI at their EC$_{50}$ concentrations could significantly inhibit the baclofen response, and the effects were additive. Bars represent the mean $\pm$ S.E.M. of 5 to 14 cells. **, $p < 0.01$, and ***, $p < 0.005$, versus vehicle control; #, $p < 0.05$, E$_2$ or DOI versus DOI plus E$_2$.

Expression of 5-HT_2 Receptor mRNA Transcripts in Arcuate (POMC) Neurons from GDX Guinea Pigs. Based on our electrophysiology results, we examined which serotonin receptors are expressed in arcuate (POMC) neurons in the guinea pig. Previous findings have identified 5-HT_{2C} receptors in male mouse POMC neurons (Heisler et al., 2002). Using scRT-PCR, we measured 5-HT_{2C}, 5-HT_{2A}, and 5-HT_{1A} receptor transcripts in 54 male and 57 female arcuate neurons, including POMC neurons from 4 animals each (Fig. 6a). Overall, the distribution of these receptors in arcuate neurons was similar in male (69 ± 13, 47 ± 6, and 51 ± 8%; $n = 4$) and female neurons (81 ± 12, 62 ± 8, and 37 ± 6; $n = 4$) for 5-HT_{2C}, 5-HT_{2A}, and 5-HT_{1A} receptors, respectively. Based on the frequency of distribution of 5-HT_{2C}, 5-HT_{2A}, and 5-HT_{1A} receptor mRNAs specifically in POMC-positive neurons in GDX female guinea pigs ($n = 38$ cells), 84% of these neurons expressed 5-HT_{2C} receptor mRNA, 76% expressed 5-HT_{2A} receptor mRNA, and 42% expressed 5-HT_{1A} receptor mRNA (Fig. 6b). The degree of coexpression of these receptors in POMC neurons was also determined as illustrated in Fig. 6b and was found to be 71% for 5-HT_{2A} and 5-HT_{2C} and 26% for all three receptors (Fig. 6b). Using RT and real-time PCR to quantify the level of expression of serotonin receptor mRNAs in the microdissected arcuate nucleus, we found that 5-HT_{2A} receptors were most highly expressed followed by 5-HT_{2C} receptors (Fig. 6, c–f; $p < 0.05$). The expression of 5-HT_{1A} was significantly lower than that of 5-HT_{2A} and 5-HT_{2C} receptor transcripts ($p < 0.001$; Fig. 6, c–f). Therefore, the scRT-PCR and qPCR data support the electrophysiological data that 5-HT_{2C} and 5-HT_{2A} receptors are highly expressed in the arcuate and coexpressed in the majority of POMC neurons.

Discussion

In the present study, we have characterized the signaling pathway of the serotonin 5-HT_{2C} receptor in hypothalamic (POMC) arcuate neurons. Activation of this Gα_q-coupled receptor desensitized the $GABA_B$ response in neurons. Short-term activation of the mER with E_2 also desensitized the $GABA_B$ receptor response, but unlike the mER signaling pathway, the 5-HT_{2C} receptor pathway led to direct hydrolysis of PIP_2 to affect GIRK channel function. Although there was a clear gender difference in the efficacy of E_2 to activate mER, there was no difference in the 5-HT_{2C}-mediated response between male and female guinea pigs. Finally, E_2 and the 5-HT_{2C} agonist DOI, albeit at a higher dose, were effective in reducing food intake and body weight gain in fasted, GDX female guinea pigs, which highlights the physiological importance of the mER and 5-HT_{2C} signaling pathways in mediating POMC neuronal excitability.

Serotonin affects arcuate (POMC) neuronal activity through multiple receptor-mediated mechanisms. Both 5-HT_{2A} and 5-HT_{2C} receptors are localized to the medial basal hypothalamus, and activation of these Gα_q-coupled receptors excites these neurons (Wright et al., 1995; Heisler et al., 2002). In particular, POMC neurons are excited in response to *d*-fenfluramine, 5-HT, or 5-HT_{2C} receptor agonists like *m*-CPP and MK212 (Heisler et al., 2002). However, the underlying mechanism(s) for the excitation of hypothalamic neurons has not been elucidated. Our data show that the Gα_q/PLC-coupled pathway of 5-$HT_{2A/C}$ receptors causes an inhibition of the baclofen response, and we provide the first evidence that depletion of PIP_2, rather than the phosphorylation of the channel, is a key step in this pathway

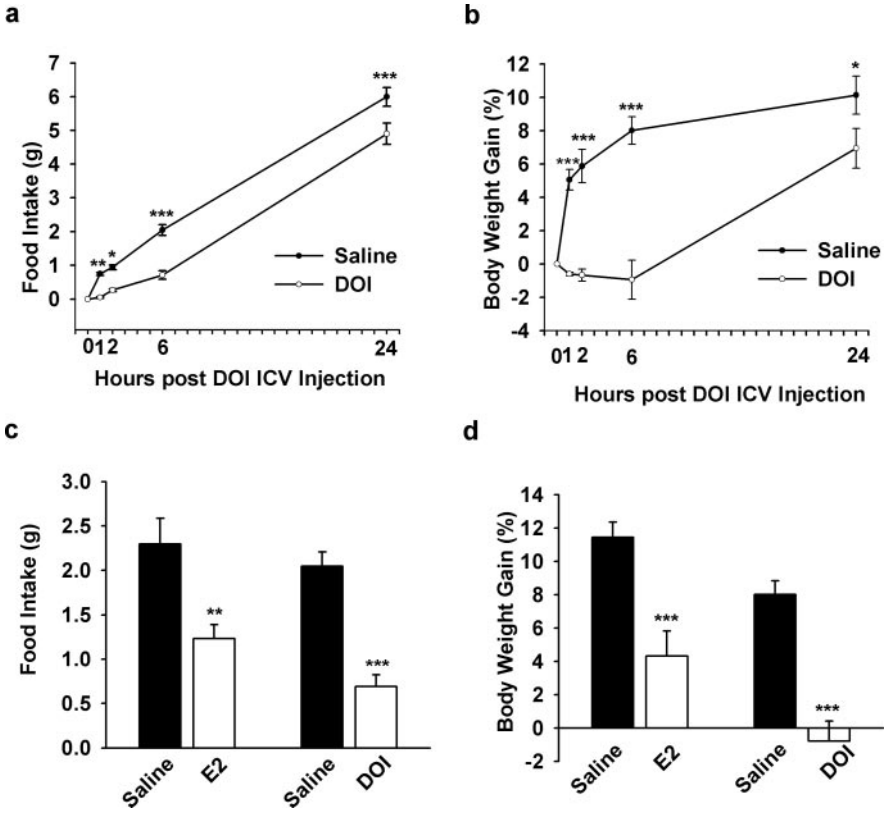

Fig. 5. 5-$HT_{2A/C}$ receptor agonist and estrogen inhibit feeding in GDX female mice. a, 5-$HT_{2A/C}$ receptor agonist DOI reduces food intake in GDX female mice. DOI (110 nmol) given icv to overnight food-deprived, ovariectomized mice produced a potent inhibition of cumulative food intake. Data are shown as means ± S.E.M., $n = 6$ for each group. *, $p < 0.05$, **, $p < 0.01$, and ***, $p < 0.005$, compared with saline vehicle-treated mice at all time points measured (two-way ANOVA and Bonferroni post test). b, 5-$HT_{2A/C}$ receptor agonist DOI reduced body weight gain in GDX female mice. DOI (110 nmol) given icv to overnight food-deprived GDX female mice produced a potent inhibition of body weight gain. Data are shown as mean ± S.E.M., $n = 6$ for each group. *, $p < 0.05$, ***, $p < 0.005$, compared with saline vehicle-treated mice at all time points measured (two-way ANOVA and Bonferroni post test). c and d, E_2, similar to DOI, reduced feeding at the 6-h time point. Bar graphs summarizing the effects of DOI and E_2 (0.012 nmol) on food intake (c) and body weight gain (d). Bars represent the mean ± S.E.M., $n = 5$ to 7 mice per group; ***, $p < 0.005$, **, $p < 0.01$, DOI or E_2 group versus their respective control groups.

based on the following: First, PKC inhibitors did not block the inhibition of the baclofen response by the 5-HT$_{2A/C}$ receptor agonist DOI or 5-HT$_{2C}$ receptor agonist *m*-CPP. Second, the DOI-mediated reduction of the GABA$_B$ response was significantly attenuated by the PLC inhibitor U73122 compared with cells perfused with the less active inhibitor U73343. Third, whole-cell dialysis with PIP$_2$ attenuated the DOI inhibition of the GABA$_B$ response, and the addition of wortmannin greatly potentiated the inhibition of DOI on baclofen responses. Finally, intracellular dialysis with a peptide fragment of Gα_q abrogated the 5-HT$_{2C}$ receptor interaction with G-protein, which indicates that 5-HT$_{2A/C}$ receptors are specifically coupled to Gα_q protein. Thus, we conclude that 5-HT$_{2A/C}$ receptor-mediated inhibition of GIRK channels involves PLC activation by Gα subunits of the Gα_q family and that the receptor-mediated hydrolysis of plasma membrane PIP$_2$ is the critical mediator. It is worth noting that although both 5-HT$_{2A}$ and 5-HT$_{2C}$ receptors are Gα_q-coupled, the inhibition of the baclofen response in POMC neurons is mainly through the 5-HT$_{2C}$ receptor because the

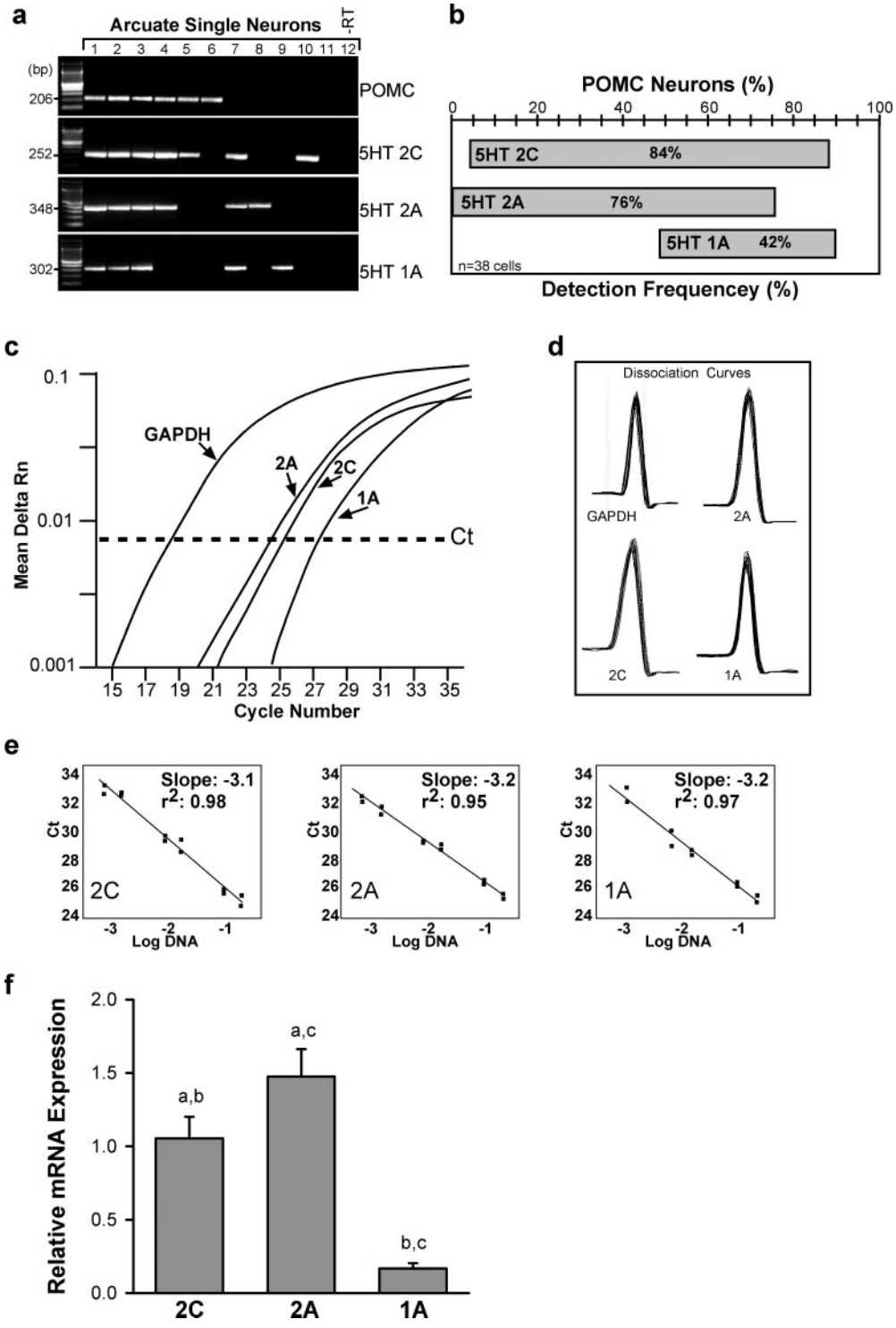

Fig. 6. 5-HT$_{2C}$ receptor mRNA is highly expressed in POMC neurons. a, representative gel illustrating the mRNA expression of 5-HT$_{2C}$, 5-HT$_{2A}$, and 5-HT$_{1A}$ receptors in arcuate neurons. All neurons expressed GAPDH (data not shown). One cell contained no MLVRT as a negative control (−RT). Other controls included aCSF from the vicinity of the harvested cells and a water blank (data not shown). b, diagram showing the distribution and coexpression of 5-HT$_{2C}$, 5-HT$_{2A}$, and 5-HT$_{1A}$ receptor transcripts in arcuate POMC neurons from GDX female guinea pigs. 5-HT$_{2C}$ and 5-HT$_{2A}$ were detected in the majority of POMC neurons, 84 and 76% respectively, whereas 5-HT$_{1A}$ receptor mRNA was detected in only 42% of POMC neurons. c, qPCR analysis of 5-HT$_{2C}$, 5-HT$_{2A}$, and 5-HT$_{1A}$ receptor mRNA expression in the microdissected arcuate nucleus using the SYBR green method. Cycle number is plotted against the normalized fluorescence intensity (Mean Delta Rn) to visualize the PCR amplification. The cycle threshold (Ct) value (broken line) is the point in the amplification at which the sample values were calculated. d, the superimposed melting curves for GAPDH, 5-HT$_{2A}$, 5-HT$_{2C}$, and 5-HT$_{1A}$ depict a single product. e, the standard curve regression line produced slope values of −3.1, −3.2, and −3.2, which translate into similar efficiencies of 100%. f, quantitative analysis of 5-HT$_{2C}$, 5-HT$_{2A}$, and 5-HT$_{1A}$ receptor mRNA expression in the arcuate nucleus from oil-treated GDX female guinea pigs (mean ± S.E.M.; $n = 6$). 5-HT$_{2A}$ and 5-HT$_{1A}$ are compared with 5-HT$_{2C}$ (one-way ANOVA: a, $p < 0.05$; b, $p < 0.001$; c, $p < 0.001$).

5-HT_{2C}-selective agonists *m*-CPP and MK212 attenuated baclofen responses in POMC neurons. Moreover, the selective 5-HT_{2C} antagonists ORG 3363 and RS102221 but not the 5-HT_{2A} antagonist spiperone potently blocked the actions of DOI in guinea pig arcuate (POMC) neurons, indicating that the inhibition of the $GABA_B$ response is through the 5-HT_{2C} receptor. This is compatible with previous findings that the 5-HT_{2C} receptor agonists show greater efficacy for activating the PLC pathway, whereas 5-HT_{2A} receptor agonists have relatively greater efficacy for activating the phospholipase A_2 pathway (Berg et al., 1998; Kurrasch-Orbaugh et al., 2003). The PLC hydrolysis of PIP_2 and inhibition of GIRK channels is not unique to 5-HT_{2C} receptors because other $G\alpha_q$-coupled receptors have different propensities for activating this pathway depending on the subcellular localizations of the G-protein-coupled receptor relative to the proximity of PLC and GIRK channels (Cho et al., 2005).

It is interesting that $GABA_B$, μ-opioid, and 5-HT_{1A} receptors are all expressed in POMC neurons (Kelly et al., 1992; Lagrange et al., 1994; Qiu et al., 2003; present findings). All of these receptors are $G\alpha_{i/o}$-coupled to activation of GIRK channels, which uniformly inhibit POMC neuronal activity. Similar to our findings with the 5-HT_{2C} receptor-mediated desensitization of the $GABA_B$ response in POMC neurons, activation of 5-HT_{2A} receptors can desensitize 5-HT_{1A} receptors and increase the excitability of CRH neurons, as measured by ACTH release (Zhang et al., 2001). The heterologous desensitization in these paraventricular nucleus neurons has not been characterized but may be via PKC-mediated phosphorylation of GIRK channels (Brown et al., 2005) or by PLC-mediated PIP_2 depletion (Brown et al., 2005; Cho et al., 2005). Therefore, the PLC-mediated PIP_2 depletion maybe a common signaling pathway for 5-$HT_{2A/C}$ receptors in hypothalamic neurons.

Evidence from several species indicates that food intake and body weight are influenced both by changes in endogenous estrogens and by exogenous estrogenic treatments (Czaja and Goy, 1975). Butera and Czaja (1984) have shown that the anorexigenic effects of E_2 are attributable to the direct actions of the steroid in the arcuate-ventromedial hypothalamic nuclei, and recently, we have shown that E_2 and STX, a selective ligand for the mER, attenuated the weight gain in female guinea pigs after ovariectomy (Qiu et al., 2006). The present findings with icv administration of E_2 in GDX female mice corroborate the findings in the guinea pig for a central action of steroid to regulate energy homeostasis. Therefore, this membrane-delimited signaling pathway may play a vital role in the control of energy homeostasis. It is interesting that eating disorders are much more prevalent (95%) in young women compared with men, but the reasons for this difference are not clear (Södersten et al., 2006). In animal models, there are clear gender differences in food intake and energy homeostasis with hormone treatment. Estrogen reduces food intake and body weight in female and

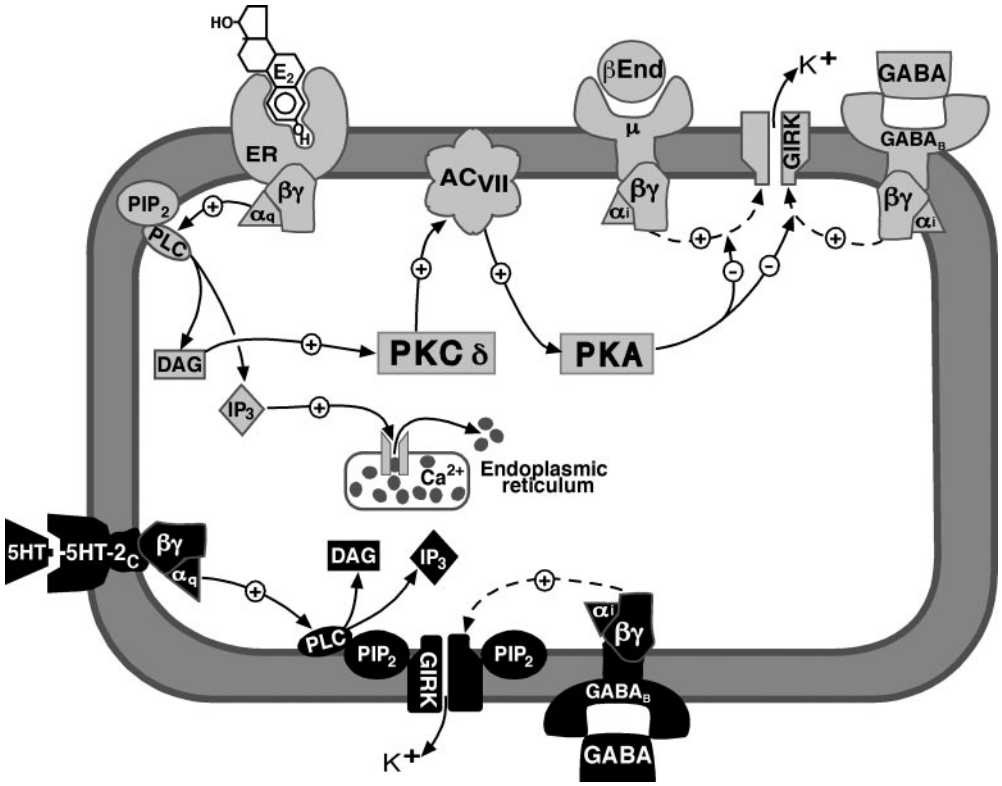

Fig. 7. A cellular model of the rapid signaling of E_2 and 5-HT in hypothalamic neurons. Schematic overview showing the mER and 5-$HT_{2A/C}$ receptor-mediated modulation of neurotransmitter regulated, G protein-coupled receptors in arcuate (POMC) neurons. Black is used to summarize the results of the current experiments. The cellular cascade activated by E_2 (Qiu et al., 2003) is shown in gray. E_2 activates a mER that is $G\alpha_{q/11}$-coupled to activation of PLC that catalyzes the hydrolysis of membrane-bound PIP_2 to IP_3 and DAG. Calcium is released from intracellular stores (endoplasmic reticulum) by IP_3, and DAG activates PKCδ. Through phosphorylation, adenylyl cyclase VII (ACVII) activity is up-regulated by PKCδ. The generation of cAMP activates PKA, which can rapidly uncouple $GABA_B$ and μ-opioid (μ) receptors from their effector system through phosphorylation of a downstream effector molecule (e.g., the inwardly rectifying K^+ channel, or GIRK). 5-HT_{2C} receptor-mediated inhibition of GIRK channels involves PLC activation by $G\alpha$ subunits of the $G_{q/11}$ family, and receptor-mediated hydrolysis of plasma membrane PIP_2 (PIP_2 depletion) is the critical mediator. Therefore, 5-HT_{2C} receptor and mER intracellular signaling pathways converge to disinhibit arcuate (POMC) neurons.

male subjects, although E_2 is more effective in female subjects and T in male subjects (Czaja and Goy, 1975; Czaja, 1984). We found that T at a higher concentration could mimic but the nonhydrolyzable androgen DHT could not mimic the effects of E_2. Moreover, E_2 was more efficacious in female than in male arcuate (POMC) neurons, but there was no gender difference in the actions of 5-HT$_{2A/C}$ agonists. Taken together, the gender differences in the control of feeding and energy homeostasis may be due in part to a greater efficacy of E_2 in female versus male guinea pigs to disinhibit POMC neurons via the mER signaling pathway.

Serotonin 5-HT$_{2C}$ receptors have also been strongly implicated in inhibiting feeding. For example, the selective 5-HT$_{2C}$ antagonist RS102221 increases food intake and body weight when injected intraperitoneally (Bonhaus et al., 2006), and 5-HT$_{2C}$ receptor-deficient mice are hyperphagic, obese, and refractory to threshold anorexic doses of *d*-fenfluramine (Tecott et al., 1995; Vickers et al., 1999), a drug that blocks the reuptake of 5-HT and stimulates its release (Heal et al., 1998). In contrast, 5-HT$_{2A}$ receptor knockout mice do not exhibit an obesity phenotype, so one may assume that 5-HT$_{2A}$ receptors are not critically involved in energy homeostasis (Zhou et al., 2005). We found that 5-HT$_{2C}$ mRNA was highly expressed and colocalized with 5-HT$_{2A}$ receptor in POMC neurons. This would disagree with in situ hybridization results in rhesus (female) monkeys showing that 5-HT$_{2C}$ receptor mRNA is highly expressed in the arcuate region, whereas the 5-HT$_{2A}$ receptor mRNA is more localized to the PVN (Gundlah et al., 1999). In addition, Heisler et al. (2002) found that up to 80% of POMC neurons express 5-HT$_{2C}$ receptor mRNA. However, the role of the 5-HT$_{2C}$ and 5-HT$_{2A}$ receptors in different physiological processes may lie in their coupling to distinctive signaling pathways.

Based on our cellular electrophysiological data, we have proposed a model for the convergence of the mER and 5-HT$_{2C}$ signaling pathways in arcuate (POMC) neurons (Fig. 7). It is noteworthy that the downstream signaling pathway of baclofen inhibition by 5-HT$_{2C}$ receptor agonists in arcuate (POMC) neurons is different from mER in which E_2 desensitizes the GABA$_B$ response via a Gα_q-PLC-PKCδ-PKA pathway (Qiu et al., 2003). These differences may be due to the different compartmentalization of the receptors. It has been reported that the signaling components for G-protein activation in neurons are compartmentalized or preassembled (Lober et al., 2006). G-protein-coupled receptors, G-proteins, and other effector molecules can preassemble into stable signaling complexes (Rebois and Hebert, 2003). Therefore, the 5-HT$_{2C}$ receptor and mER may be preassembled into complexes with different downstream effectors that converge on GIRK channels. For example, Brown and colleagues (2005) have shown that although protein kinases (i.e., PKCδ) mediate the inhibition of GIRK$_{1/2}$ channels by the muscarinic M_3 receptor, resynthesis of PIP_2 is required for complete recovery from inhibition. Therefore, PIP_2 turnover is critical for GIRK channel function. Our data support this idea because 5-HT$_{2C}$ receptors can inhibit the GIRK channels by an independent pathway from mER, but the two pathways converge on the same population of GIRK channels as shown by the additive effects of the two agonists given together. As proof of principle, we have found that both E_2 and DOI are effective to inhibit feeding in GDX female mice, and as predicted from the cellular findings, E_2 was more potent than DOI to inhibit food intake and weight gain. Therefore, the Gα_q signaling pathways of mER and 5-HT$_{2C}$ receptors may converge to enhance synaptic efficacy in brain circuits that are critical for maintaining homeostatic functions.

Acknowledgments

We recognize the skilled technical assistance of Rebecka Amodei and Scott Kuhn. We recognize Dr. Jan Kelder (Organon NV) for his generous gift of ORG 3363.

References

Berg KA, Maayani S, Goldfarb J, and Clarke WP (1998) Pleiotropic behavior of 5-HT2$_A$ and 5-HT2$_C$ receptor agonists. *Ann N Y Acad Sci* **861:**104–110.

Bethea CL (1993) Colocaliztion of progestin receptors with serotonin in Raphe neurons of Macaque. *Neuroendocrinology* **57:**1–6.

Bethea CL, Pecins-Thompson M, Schutzer WE, Gundlah C, and Lu ZN (1998) Ovarian steroids and serotonin neural function. *Mol Neurobiol* **18:**87–123.

Bickerdike MJ (2003) 5-HT2$_C$ receptor agonists as potential drugs for the treatment of obesity. *Curr Top Med Chem* **3:**885–897.

Bonhaus SJ, Weinhardt KK, Taylor M, DeSouza A, McNeeley PM, Szczepanski K, Fontan DJ, Trinh J, Rocha CL, and Dawson MW (2006) RS-102221: a novel high affinity and selective, 5-HT2$_C$ receptor antagonist. *Neuropharmacology* **36:**621–629.

Breisch ST, Zemlan FP, and Hoebel BG (1976) Hyperphagia and obesity following serotonin depletion by intraventricular P-chlorophenylalanine. *Science* **192:**382–385.

Brown SG, Thomas A, Dekker LV, Tinker A, and Leaney JL (2005) PKC-δ sensitizes Kir3.1/3.2 channels to changes in membrane phospholipid levels after M_3 receptor activation in HEK-293 cells. *Am J Physiol Cell Physiol* **289:**C543–C556.

Butera PC and Czaja JA (1984) Intracranial estradiol in ovariectomized guinea pigs: Effects on ingestive behaviors and body weight. *Brain Res* **322:**41–48.

Carr DB, Cooper DC, Ulrich SL, Spruston N, and Surmeier DJ (2002) Serotonin receptor activation inhibits sodium current and dendritic excitability in prefrontal cortex via a protein kinase C-dependent mechanism. *J Neurosci* **22:**6846–6855.

Cepoi D, Phillips T, Cismowski M, Goodfellow VS, Ling N, Cone RD, and Fan W (2004) Assessment of a small molecule melancortin-4 receptor-specific agonist on energy homeostasis. *Brain Res* **1000:**64–71.

Cho H, Lee D, Lee SH, and Ho WK (2005) Receptor-induced depletion of phosphatidylinositol 4,5-bisphosphate inhibits inwardly rectifying K^+ channels in a receptor-specific manner. *Proc Natl Acad Sci U S A* **102:**4643–4648.

Cone RD (2005) Anatomy and regulation of the central melanocortin system. *Nat Neurosci* **8:**571–578.

Conn PJ, Sanders-Bush E, Hoffman B, and Hartig PR (1986) A unique serotonin receptor in choroid plexus is linked to phosphatidylinositol turnover. *Proc Natl Acad Sci U S A* **83:**4086–4088.

Couse JF and Korach KS (1999) Estrogen receptor null mice: What have we learned and where will they lead us? *Endocr Rev* **20:**358–417.

Czaja JA (1984) Sex differences in the activational effects of gonadal hormones on food intake and body weight. *Physiol Behav* **33:**553–558.

Czaja JA and Goy RW (1975) Ovarian hormones and food intake in female guinea pigs and Rhesus monkeys. *Horm Behav* **6:**329–349.

de Chaffoy de Courcelles D, Leysen JE, de Clerck F, Van Belle H, and Janssen PA (1985) Evidence that phospholipid turnover is the signal transducing system coupled to serotonin-S2 receptor sites. *J Biol Chem* **260:**7603–7608.

Elmquist JK, Elias CF, and Saper CB (1999) From lesions to leptin: hypothalamic control of food intake and body weight. *Neuron* **22:**221–232.

Franklin KBJ and Paxinos G (1997) *Atlas of the Mouse Brain.* Academic Press, San Diego, CA.

Gropp E, Shanabrough M, Borok E, Xu AW, Janoschek R, Buch T, Plum L, Balthasar N, Hampel B, Waisman A, et al. (2005) Agouti-related peptide-expressing neurons are mandatory for feeding. *Nat Neurosci* **8:**1289–1291.

Gundlah C, Pecins-Thompson M, Schutzer WE, and Bethea CL (1999) Ovarian steroid effects on serotonin 1A, 2A and 2C receptor mRNA in Macaque hypothalamus. *Mol Brain Res* **63:**325–339.

Heal DJ, Cheetham SC, Prow MR, Martin KF, and Buckett WR (1998) A comparison of the effects on central 5-HT function of sibutramine hydrochloride and other weight-modifying agents. *Br J Pharmacol* **125:**301–308.

Heisler LK, Cowley MA, Tecott LH, Fan W, Low MJ, Smart JL, Rubinstein M, Tatro JB, Marcus JN, Holstege H, et al. (2002) Activation of central melanocortin pathways by fenfluramine. *Science* **297:**609–611.

Heisler LK, Jobst EE, Sutton GM, Zhou L, Borok E, Thornton-Jones Z, Liu HY, Zigman JM, Balthasar N, Kishi T, et al. (2006) Serotonin reciprocally regulates melanocortin neurons to modulate food intake. *Neuron* **51:**239–249.

Kelly MJ, Loose MD, and Rønnekleiv OK (1992) Estrogen suppresses μ-opioid and GABA$_B$-mediated hyperpolarization of hypothalamic arcuate neurons. *J Neurosci* **12:**2745–2750.

Kelly MJ and Rønnekleiv OK (1994) Electrophysiological analysis of neuroendocrine neuronal activity in hypothalamic slices, in *Methods in Neurosciences: Pulsatility in Neuroendocrine Systems* (Levine JE ed) pp 47–67, Academic Press, Inc., San Diego.

Kurrasch-Orbaugh DM, Watts VJ, Barker EL, and Nichols DE (2003) Serotonin 5-hydroxytryptamine 2A receptor-coupled phospholipase C and phospholipase A2 signaling pathways have different receptor reserves. *J Pharmacol Exp Ther* **304:**229–237.

Lagrange AH, Rønnekleiv OK, and Kelly MJ (1994) The potency of μ-opioid hyper-

polarization of hypothalamic arcuate neurons is rapidly attenuated by 17β-estradiol. *J Neurosci* **14:**6196–6204.

Livak KJ and Schmittgen TD (2001) Analysis of relative gene expression data using real-time quantitative PCR and the $2^{-\Delta\Delta C_T}$ method. *Methods* **25:**402–408.

Lober RM, Pereira MA, and Lambert NA (2006) Rapid activation of inwardly rectifying potassium channels by immobile G-protein-coupled receptors. *J Neurosci* **26:**12602–12608.

Luquet S, Perez FA, Hnasko TS, and Palmiter RD (2005) NPY/AgRP neurons are essential for feeding in adult mice but can be ablated in neonates. *Science* **310:**683–685.

McEwen BS (2001) Estrogens effects on the brain: Multiple sites and molecular mechanisms. *J Appl Physiol* **91:**2785–2801.

Pfaffl MW (2001) A new mathematical model for relative quantification in real-time RT-PCR. *Nucleic Acids Res* **29:**e45.

Qiu J, Bosch MA, Tobias SC, Grandy DK, Scanlan TS, Rønnekleiv OK, and Kelly MJ (2003) Rapid signaling of estrogen in hypothalamic neurons involves a novel G protein-coupled estrogen receptor that activates protein kinase C. *J Neurosci* **23:**9529–9540.

Qiu J, Bosch MA, Tobias SC, Krust A, Graham S, Murphy S, Korach KS, Chambon P, Scanlan TS, Rønnekleiv OK, et al. (2006) A G protein-coupled estrogen receptor is involved in hypothalamic control of energy homeostasis. *J Neurosci* **26:**5649–5655.

Rebois RV and Hebert TE (2003) Protein complexes involved in heptahelical receptor-mediated signal transduction. *Receptors Channels* **9:**169–194.

Södersten P, Bergh C, and Zandian M (2006) Understanding eating disorders. *Horm Behav* **50:**572–578.

Stearns V, Ullmer L, Lopez JF, Smith Y, Isaacs C, and Hayes DF (2002) Hot flushes. *Lancet* **360:**1851–1861.

Tecott LH, Sun LM, Akana SF, Strack AM, Lowenstein DH, Dallman MF, and Julius D (1995) Eating disorder and epilepsy in mice lacking 5-HT2C serotonin receptors. *Nature* **374:**542–546.

Vickers SP, Clifton PG, Dourish CT, and Tecott LH (1999) Reduced satiating effect of d-fenfluramine in serotonin 5-HT_{2C} receptor mutant mice. *Psychopharmacology (Berl)* **143:**309–314.

Wright DE, Seroogy KB, Lungren KH, Davis BM, and Jennes L (1995) Comparative localization of serotonin 1A, 1C, and 2 receptor subtype mRNAs in rat brain. *J Comp Neurol* **351:**357–373.

Zhang Y, D'Souza D, Raap DK, Garcia F, Battaglia G, Muma NA, and Van de Kar LD (2001) Characterization of the functional heterologous desensitization of hypothalamic 5-HT_{1A} receptors after 5-HT_{2A} receptor activation. *J Neurosci* **21:**7919–7927.

Zhou L, Williams T, Lachey JL, Kishi T, Cowley MA, and Heisler LK (2005) Serotonergic pathways converge upon central melanocortin systems to regulate energy balance. *Peptides* **26:**1728–1732.

Address correspondence to: Dr. Jian Qiu, Department of Physiology and Pharmacology, L334, Oregon Health and Science University, Portland, OR 97239-3098. E-mail: qiuj@ohsu.edu